Res Chem Intermed (2015) 41:2221–2233
DOI 10.1007/s11164-013-1340-8

Regioselective acylation of methyl-α-D-glucopyranoside with different acylating agents catalysed by micro/mesoporous materials

Bouhadjar Boukoussa · Fatiha Sebih · Rachida Hamacha · Salima Bellahouel · Aicha Derdour · Abdelkader Bengueddach

Received: 7 April 2013 / Accepted: 12 July 2013 / Published online: 30 July 2013

Abstract The composite microporous/mesoporous material ZSM-5/MCM-48 was successfully prepared by hydrothermal synthesis using a simple one-step crystallization process. The material was a mesoporous composite containing zeolite and crystals of ZSM-5. The textural and structural features of this material were characterized by use of powder XRD, nitrogen sorption, FTIR spectroscopy, SEM, and TEM. The mesoporous material obtained, Al-MCM-48, and the composite material, ZSM-5/MCM-48, were used as catalysts for acylation of methyl-α-D-glucopyranoside. Fatty acids ($n = 10$, 14, and 16) and fatty acid chlorides were used, individually, as acylating agents for this reaction. The effects of solvent, type of catalyst, and nature of the fatty acids on the acylation reaction were investigated. Reaction yields in the range 50–70 % were achieved by use of this synthetic pathway. The products resulting from the acylation reaction are new nonionic biosurfactants.

Keywords Mesoporous materials · Composite materials · Chemical esterification · Carbohydrates · Selective acylation

Introduction

Synthesis of the new family of mesoporous M41S materials was first reported by Kresge et al. [1] and Beck et al. [2]. They are very attractive materials because of their narrow pore-size distributions (from 2–10 nm) and their large surface areas

B. Boukoussa (✉) · R. Hamacha · A. Bengueddach
Laboratoire de chimie des matériaux L.C.M, Université d'Oran, BP, 1524 Oran El-Mnaouer, Algérie
e-mail: bbouhdjer@yahoo.fr

F. Sebih · S. Bellahouel · A. Derdour
Laboratoire de Synthèse Organique Appliquée L.S.O.A, Université d'Oran,
BP, 1524 Oran El-Mnaouer, Algérie

(>1,000 m^2/g) [3]. They are nontoxic and highly biocompatible [4–6]. Because of their specific and interesting features these mesoporous materials are widely used in a large number of industrial applications, e.g., as catalysis [7, 8], for separation [9, 10] and adsorption [11], in photoluminescent products [12], in the electrochemical [13] and energy [14] industries, and as drug-delivery systems [15]. Because of their amorphous structures, the hydrothermal stability, ion-exchange capacity, and acidity of mesoporous materials are usually poor compared with the crystalline zeolites. Recently, much research effort has been devoted to improving the hydrothermal stability and acidity of mesoporous aluminosilicates. One approach used is partial crystallization of the amorphous pore walls [16, 17]. Owing to its three dimensional structure and the accessibility of its pores MCM-48 has become the most popular mesoporous material in catalysis, separation, and adsorption processes. Xia and Mokaya, obtained zeolite/MCM-48 by use of a simple two-step crystallisation process [18, 19]. Prokesova et al. [20, 21] prepared composites by simultaneous hydrothermal treatment of an MCM-48 precursor solution and a colloidal solution containing amorphous zeolite seeds. Li et al. [22] reported a simple one-step hydrothermal procedure for synthesis of stable mesoporous materials with a highly ordered cubic structure. These micro/mesoporous materials have high catalytic performance in numerous chemical reactions, e.g. palm oil cracking [23], acylation of anisole with octanyl chloride [24], formation of aromatic hydrocarbons in the conversion of methanol to gasoline [25], esterification of acetic acid with *n*-butyl alcohol [26], and oxidation of benzene [27, 28].

Carbohydrate fatty acid esters are synthesized either chemically or enzymatically. The chemical method is often complicated by poor reaction selectivity which leads to undesirable side reactions and low yields [29, 30]. In recent years, methods based on enzyme-catalysed synthesis of sugar derivatives have been developed [31–33]. Regio and stereo-selective products have been obtained enzymatically and the products were compared with those obtained by use of classical chemistry. Recent work on carbohydrate fatty acid esters has focussed on establishing an effective regioselective and catalytic process [34]. Methyl-α-D-glucopyranoside has been used in several regioselective reactions with benzyl bromide, allyl bromide, and trityl chloride [35, 36], containing different tertiary amines [37–41], but their selectivity with fatty acids has never been achieved by using micro/mesoporous materials.

In this work, we describe a modification of the method of Sakthivel et al. [42] that enabled us to obtain micro/mesoporous composites containing zeolite secondary building units and zeolite crystals. In this method we used tetrapropylammonium hydroxide (TPAOH) instead of the classic NaOH. We developed a catalytic route using calcined and uncalcined Al-MCM-48 and composite material ZSM-5/MCM-48 that are very poorly described in the literature on regioselective synthesis of sugar fatty esters based on sugar methyl-α-D-glucopyranoside and fatty acids. The main objective was to avoid the steps of protection and deprotection usually applied, because of the presence of several hydroxyl groups of similar reactivity in sugar molecules [43]. These esters are widely used in many commercial applications, for example non-ionic surfactants in pharmaceuticals and cosmetics, because they are biodegradable, non-toxic, and non-irritant [31, 44].

Experimental

Preparation of ZSM-5/MCM-48 composite materials and Al-MCM-48

The synthetic method was similar to that described by Sakthivel et al. [42]. The modification made was the molar composition of the gel. ZSM-5/MCM-48 materials with molar gel composition 1 SiO_2, 0.14 CTAB, 0.00625 Al_2O_3, 0.75 TPAOH, and 75 H_2O, were synthesized by a one-step method in which TPAOH was used instead of NaOH. A homogeneous surfactant solution was prepared by dissolving CTAB in water at 35 °C and an appropriate amount of the silica source was added. The resulting mixture was stirred for 15 min. A solution containing aluminium and TPAOH was then added, and the resulting gel was stirred between 2 and 4 h at 35 °C to enable formation of the microporous/mesoporous phase. The synthesized gel was transferred to an autoclave where it was heated at 100 °C for 72 h. The uncalcined solid product was recovered by filtration, dried in open air, and calcined at 550 °C for 6 h to remove any traces of organic additives. For comparison with the catalytic activity of ZSM-5/MCM-48 we synthesized Al-MCM-48 by the method of Yong de Xia et al. [45]. Two different Si/Al ratios (Si/Al = 80 and 40) were incorporated into the structure of Al-MCM-48.

Characterization

Powder X-ray diffraction (XRD) patterns of samples dried at 353 K were collected at room temperature on a Bruker AXS D-8 diffractometer with Cu Ka radiation. Nitrogen adsorption experiments were performed at 77 K on a Micromeritics TriStar 3000 V6.04 A. Samples were out-gassed at 353 K before adsorption measurements until a 3×10^{-3} Torr static vacuum was reached. The surface area was calculated by use of the Brunauer–Emmett–Teller (BET) method and the distribution of the pores was evaluated by use of the BJH method [46]. FT-IR spectra of the microporous/mesoporous materials in the range 400–4,000 cm^{-1} were acquired with a Jasco 4200 instrument using the KBr pellet technique. Approximately 10 mg sample was ground with approximately 200 mg spectral-grade KBr to form a pellet under hydraulic pressure. Scanning electron microscopy (SEM) was performed with an Hitachi 4800S microscope. Transmission electron microscopy (TEM) was performed with a Jeol 1200 EXII.

Acylation of methyl-α-D-glucopyranoside

Fifteen millilitres of a mixture containing equimolar (typically 1 mol) amounts of methyl-α-D-glucopyranoside and fatty acid or fatty acid chloride, were added to 15 ml DMF. The mixture was stirred at 333 K on an oil bath under nitrogen. Reaction was initiated by adding 0.01 g catalyst to the mixture. After 72 h, samples of methyl-α-D-glucopyranoside and methyl-α-D-glucopyranoside ester from the reacting mixture were analysed by thin-layer chromatography (TLC). The reaction product was filtered to eliminate the catalyst then the DMF was evaporated. The product was applied to a silica gel column and eluted with chloroform and ethanol

(13:3, *v*/*v*). The purified sample was subjected to further analysis and characterization (^{1}H NMR and ^{13}C NMR). The fatty acids tested in this synthesis were lauric, palmitic, stearic, and palmitic acids; the acid chlorides were palmitic acid chloride and lauric acid chloride.

Results and discussion

Characterization of micro/mesoporous composite materials and Al-MCM-48

Figure 1a shows the XRD patterns of calcined and uncalcined ZSM-5/MCM-48 materials. It is clear that both materials have distinctive XRD patterns. When the zeolite precursor species were formed, the XRD pattern of the resulting material (sample ZSM-5/MCM-48) had a basal peak (211) and several other peaks, which are attributed to the cubic (Ia3d) MCM-48. The XRD pattern of ZSM-5/MCM-48 therefore indicates that a structurally well ordered cubic MCM-48 aluminosilicate was successfully assembled from ZSM-5 zeolite seeds. Extending the aging time of the zeolite precursor species between 2 and 4 h results in the formation of a composite material composed of a cubic MCM-48 phase and ZSM-5 zeolite. This is clear evidence of the formation of zeolite building units. Most of the SBU formed the MCM-48 composite whereas a small amount led to the formation of crystals of zeolite ZSM-5. Figure 1b shows the XRD patterns of calcined Al-MCM-48 with different Si/Al ratios. All calcined samples had XRD patterns typical of well ordered mesoporous materials. An intense diffraction peak was observed at low angle and at least three higher-order peaks; these can be indexed as (211), (220), (420), and (332) reflections. These features are consistent with a well defined cubic structure, which is characteristic of Al-MCM-48. The presented XRD patterns are in good agreement with previous reports for similar materials obtained by use of differing synthetic methods [46].

The unit cell parameter of calcined Al-MCM-48 samples increased with decreasing Si/Al ratio, suggesting a decrease in wall thickness with decreasing Al content (Table 1). The results obtained by N_2 adsorption/desorption measurements (77 K) for ZSM-5/MCM-48 and Al-MCM-48 with different Si/Al ratios are presented in Fig. 2. The isotherm, i.e. the adsorption/desorption curve, of these materials was a typical type IV isotherm with a sharp inflection at $P/P_o = 0.35$ and a broad hysteresis loop, characteristic of capillary condensation in mesoporous channels. Their textural properties, such as unit cell parameter (a_0), surface area, pore size, and wall thickness are summarized in Table 1.

Barret–Joyner–Halenda (BJH) pore size distribution analysis showed that these materials have uniform mesopores with bimodal pore openings centered at approximately 38 Å (Fig. 3).

The FT-IR spectra of the uncalcined ZSM-5/MCM-48 and Al-MCM-48, given in Fig. 4, indicate the three samples have almost the same chemical structure (same IR spectrum) but with different peak intensities. The presence of absorption bands at approximately 2927 and 2852 cm^{-1} for the uncalcined materials corresponds to asymmetric and symmetric CH_2 vibrations of the surfactant molecules.

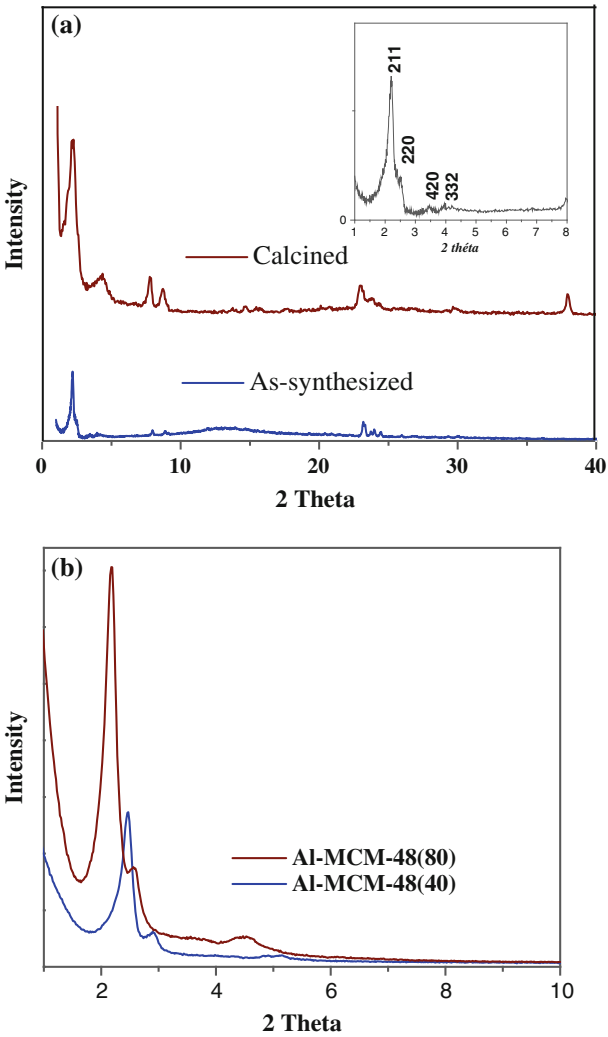

Fig. 1 Powder XRD patterns of Al-MCM-48 and ZSM-5/MCM-48 composite material. **a** ZSM-5/MCM-48 composite and **b** Al-MCM-48 with (Si/Al = 80 and 40)

Table 1 Textural properties and elemental composition of the materials studied

Samples	a_o (Å)	S_{BET} (m^2/g)	V_{meso} (cm^3/g)	D_{BJH} (Å)	H (Å)
ZSM-5/MCM-48	98	1086.68	0.72	38.16	12.6
Al-MCM-48(80)	88	815.74	0.64	38.25	9.33
Al-MCM-48(40)	96	803.63	0.63	38.53	11.78

$a_0 = d_{hkl}(h^2 + k^2 + l^2)^{1/2}$. $H = (a_0/3.092) - (D/2)$

a_0 unit cell parameter, S_{BET} BET specific surface area, D_{BJH} pore diameter, H thickness of walls

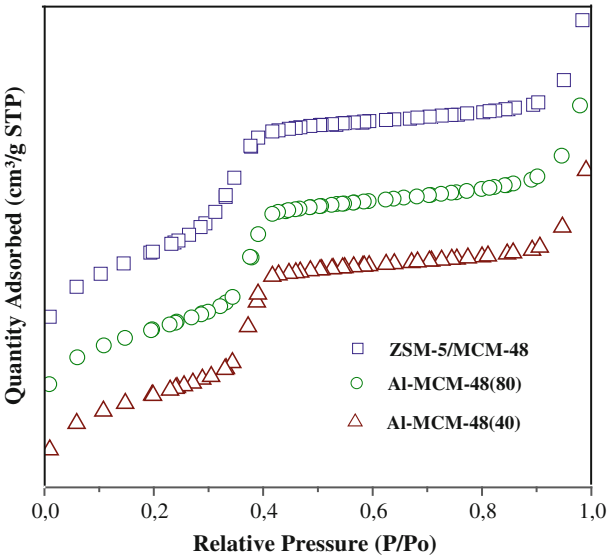

Fig. 2 Nitrogen sorption isotherms of ZSM-5/MCM-48 and Al-MCM-48

Fig. 3 BJH pore size distributions of ZSM-5/MCM-48 composite and Al-MCM-48

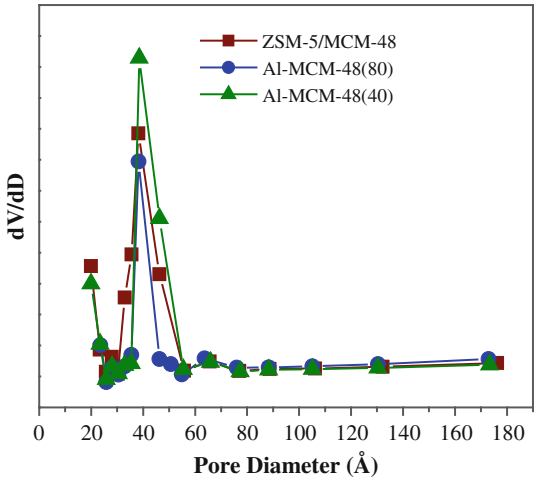

In the infrared spectrum of the uncalcined samples the broad peaks at approximately 3500 cm^{-1} are ascribed to O–H stretching of surface hydroxyl groups, bridged hydroxyl groups, and adsorbed water molecules; deformational vibrations of the adsorbed molecules cause the adsorption bands at 1626–1638 cm^{-1}. The peaks (bands) between 500 and 1200 cm^{-1} are assigned to the framework vibration. Those at approximately 1247 and 1072 cm^{-1} are attributed to the asymmetric stretching of T–O–T groups. The peaks at 800 and 544 cm^{-1} and that at 460 cm^{-1} arise from the bending mode of T–O–T. For the

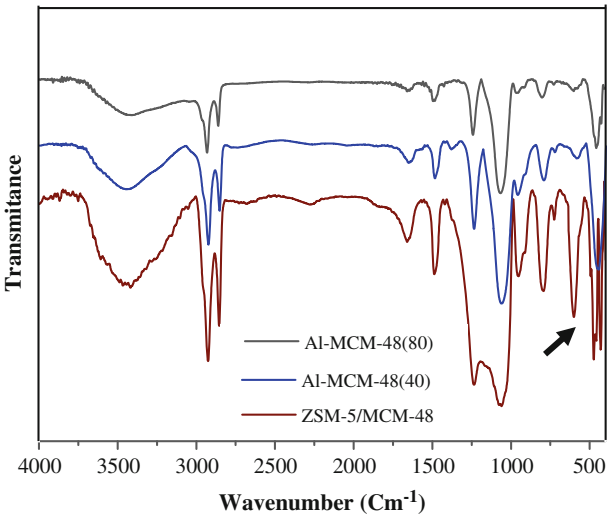

Fig. 4 FTIR spectra of ZSM-5/MCM-48 composite materials and Al-MCM-48

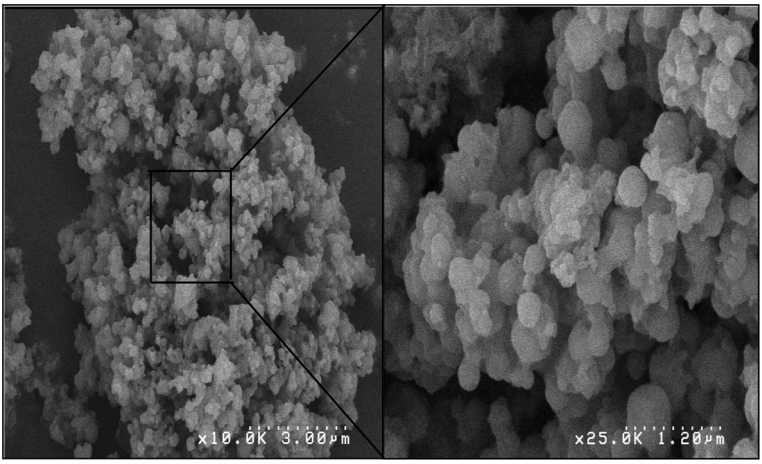

Fig. 5 SEM images of ZSM-5/MCM-48

composite material ZSM-5/MCM-48 an additional band at approximately 580 cm^{-1} is visible; this is ascribed to the presence of zeolitic secondary building units in the framework [19].

The particle morphology of the composite material ZSM-5/MCM-48 was investigated by use of scanning electron microscopy (SEM). Representative SEM images obtained for the sample ZSM-5/MCM-48 are shown in Fig. 5. The cubic phase MCM-48 sample (ZSM-5/MCM-48) is mainly made up of sub-micrometer-sized aggregated spherical particles. Larger solid shell-like particles are also observed, which is consistent with previous reports [19].

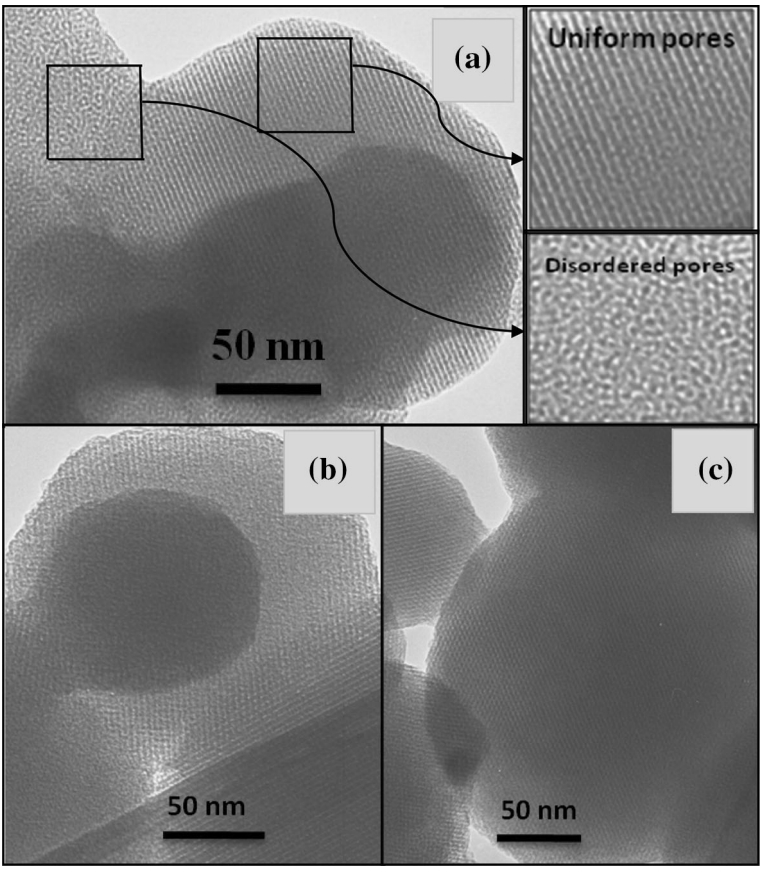

Fig. 6 TEM images: **a** composite material ZSM-5/MCM-48, **b** Al-MCM-48(80), **c** Al-MCM-48(40)

We used transmission electron microscopy (TEM) to probe the structural pore ordering and morphology of the materials. The TEM micrograph of composite material ZSM-5/MCM-48 in Fig. 6 shows that the cubic MCM-48 phase assembled from zeolite ZSM-5 seeds (ZSM-5/MCM-48) is structurally well ordered with inhomogeneous size pore channels. From the TEM micrographs an approximate channel distance of 3.5 nm can be obtained. This value is close to the pore size obtained from nitrogen sorption data (Table 1). For Al-MCM-48 with different Si/Al ratios the TEM images reveal that the distribution of pores is homogeneous and uniform.

Application of ZSM-5/MCM-48 and Al-MCM-48 in the acylation reaction

Effect of solvent

Organic solvents are important in esterification reactions, affecting not only the yield of the reaction but also positional selectivity [47–49]. The choice of solvent

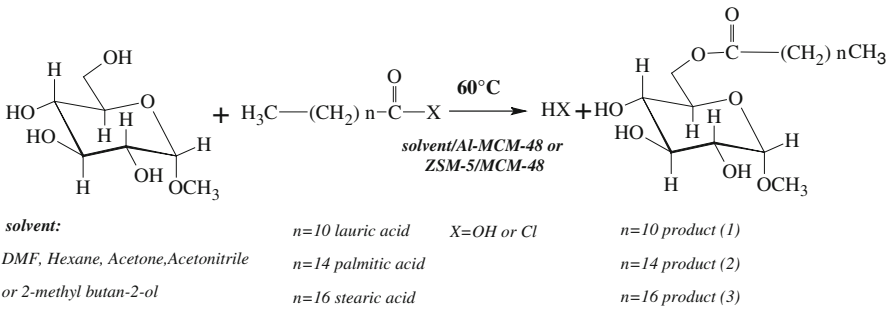

Fig. 7 Acylation of methyl-α-D-glucopyranoside with fatty acid

for esterification of carbohydrates with fatty acids is not a simple task. The solubility of sugars and fatty acids in organic solvents are usually markedly different, which complicates the esterification reaction at high concentrations of both reactants. In addition, the solvent must not adversely affect the stability of the catalyst and its activity [50].

To study the effect of solvent on the reaction of methyl-α-D-glucopyranoside with lauric acid in the presence of calcined Al-MCM-48 (Si/Al = 40), solvents of different polarity were tested. As shown in Fig. 7, dimethylformamide (DMF), hexane, acetone, acetonitrile (CH_3CN), 2-methyl butan-2-ol (amyl alcohol) were individually tested. The reaction solution was heated to 60 °C, with magnetic stirring under a nitrogen atmosphere. The yields of the expected esterified product are listed in Table 2. These results clearly indicate that the reaction gives what we regard as good yields of 48 % in the polar solvent DMF. We can explain these results by the low solubility of sugar in such organic solvents as hexane and CH_3CN. Unprotected sugars are soluble at high concentrations in a few hydrophilic solvents only, for example DMF [51]. The presence of the amyl alcohol at 60 °C for this reaction affects the silanol surface [52, 53]. Note that amyl alcohol is used to esterify and deactivate the surface in accordance with the reaction [52, 53]:

$$\equiv Si-OH + R-OH \rightarrow \equiv Si-OR + H_2O$$

Effect of catalyst

Other catalysts are used to improve the esterification reaction. As presented in Fig. 7 and listed in Table 3 different situations can be distinguished. When uncalcined mesoporous catalysts are used, the yield is usually low (26 and 22 % for Al-MCM-48 and Al-MCM-41, respectively). It is substantially increased, however, when calcined Al-MCM-48 and Al-MCM-41 with the same Si/Al ratio, Al-MCM-48(40) and Al-MCM-41(40), are used (48 and 38 % for Al-MCM-48 and Al-MCM-41, respectively). Because of its three-dimensional pore structure and its more hydrophilic nature, Al-MCM-48 is regarded as a better catalyst than Al-MCM-41 [54]. It allows faster diffusion through the channels [55]. We note that calcined and uncalcined Al-MCM-41 have different catalytic activity (38, 22 %

Table 2 Effect of the solvent in the reaction of methyl-α-D-glucopyranoside with lauric acid

Catalyst	Time (days)	Solvent	Yield (%)
Calcined Al-MCM-48(40)	3	DMF	48
Calcined Al-MCM-48(40)	5	Hexane	6
Calcined Al-MCM-48(40)	4	THF	18
Calcined Al-MCM-48(40)	3	Acetone	28
Calcined Al-MCM-48(40)	2	Acetonitrile	Trace of product <10 %
Calcined Al-MCM-48(40)	5	Amyl alcohol	0 %
Calcined ZSM-5/MCM-48	3	DMF	60

Table 3 Effect of the nature of the catalyst

Catalyst	Time (days)	Yield (%)
Calcined Al-MCM-48(80)	3	31
Uncalcined Al-MCM-48(80)	3	26
Calcined Al-MCM-48(40)	3	48
Calcined Al-MCM-41(40)	3	38
Uncalcined Al-MCM-41(40)	3	22
Calcined ZSM-5/MCM-48(80)	3	60
Uncalcined ZSM-5/MCM-48(80)	3	68
Blank test	>3	0

respectively). The low efficiency is because of pore blockage by the surfactant. Similar results have been reported showing the superiority of MCM-48 (90 % surfactant loss) to MCM-41 (70 % surfactant loss) during treatment with acid/alcohol solvent [56, 57]. These results support our findings that the reaction in MCM-48 pores was much more efficient than that in MCM-41 pores. We attribute the inefficiency of the latter to less accessible pores, because of the substantial amount of residual surfactant. However, the yield increases slightly in the presence of mesoporous Al-MCM-48 with different Si/Al ratio (48 and 31 %, respectively Si/Al = 40 and 80). This difference is attributed to variation of the Si/Al ratio. The first material is more acidic than the second. For the same reaction time, these results have been demonstrated by many researchers who studied the effect of Si/Al ratio on the esterification reaction and observed that the acidity increases with incorporation of Al into the structural lattice of the mesoporous materials [58–60]. Use of the catalyst ZSM-5/MCM-48 led to an attractive yield (60–68 %), in particular, for the uncalcined sample with pores blocked by the surfactant. Similar activity is observed whether or not the catalyst is calcined, suggesting the solvent dissolves the surfactant and releases the porosity.

Effect of acylating agent

We also repeated this reaction by reacting the methyl-α-D-glucopyranoside with lauric or palmitic acid chloride (Fig. 7). The reaction was performed in DMF at

Table 4 Effect of acylating agent

Acylating agent	Product	Yield (%)
Lauric acid chloride	1	65
Palmitic acid chloride	2	51
Lauric acid	1	60
Palmitic acid	2	48
Stearic acid	3	30

60 °C in the presence of calcined composite ZSM-5/MCM-48(80). The reaction led to products with yields of 65 and 51 %, respectively (Table 4). No significant differences in yield were observed between fatty acid chloride or fatty acid. In contrast, the results reveal that as the chain length of the fatty acid increases the yield decreases. The same behaviour was reported by Bellahouel et al. [61] for acylation of sugar (*N*-methylglucamine) with lauric, palmitic, and stearic acids and by Barrault et al. [62] for glycerol *trans*-esterification in the presence of Mg–MCM-41 catalyst.

Conclusions

We have developed a direct synthetic route for preparing micro/mesoporous aluminosilicate catalyst ZSM-5/MCM-48 via a one-step crystallization process in which NaOH was substituted by TPAOH. The main objective was to obtain relatively pure forms of both end members (zeolite ZSM-5 and zeolite seed containing MCM-48) from similar precursor zeolite solutions after appropriate aging. Acylation of methyl-α-D-glucopyranoside with different acylating agents in the presence of our catalysts were found to be very regioselective without the need for protection and deprotection steps. The micro/mesoporous composites were more reactive than Al-MCM-48, because of the presence of strong sites. Several conditions can affect the yield of product, for example the nature of the solvent, the choice of catalyst, and the nature of the acylating agent. Better yield can be achieved if protonation or grafting of acid groups has been conducted. In our work only silanol groups were involved in catalysis of the reaction.

Product (1)

$R_f = 0.2$ (MeOH/$CHCl_3$ 1/9). sulfuric acid. $T_f = 280$ °C. Chemical formula: $C_{19}H_{36}O_7$ (376).

IR (KBr, solid): ν (OH) = 3549 cm^{-1}. ν (CH) = 2852, 2919 cm^{-1}. ν (CO–O) = 1705 cm^{-1}.

^{1}H NMR, δ (ppm): ($CDCl_3$): 5.03 (d, 1H, H-1, $J^2 = 7.02$ Hz), 4,29 (m, 2H, H-6), 4.09 (m, 1H, H-5), 3,73 (m, H, H-3), 3,34–3.40 (m, 2H, H-3,4), 3,24 (s, 3H, OCH_3), 2.52 (s, 3H, 3OH), 2.25 (t, 2H, $CH_2CH_2CO_2$, $J^3 = 6.82$ Hz), 1.67 (m, 2H, $CH_2CH_2CO_2$), 1.30 (m, 16H, $(CH_2)_8$), 0.94 (t, 3H, CH_2CH_3, $J^3 = 7.08$).

^{13}C NMR ($CDCl_3$): 14.01, 22.80, 25.23, 28.9, 29.09, 31.55, 32.57, 33.37, 55.80, 60.53, 72.68, 72.71, 78.74, 79.01, 103.54, 174.27.

Product (2)

$R_f = 0.16$ (MeOH/$CHCl_3$ 1/9). sulfuric acid. $T_f = 320$ °C. Chemical formula: $C_{23}H_{44}O_7$ (432). IR (KBr, solid): ν (OH) = 3540 cm^{-1}. ν (CH) = 2852, 2919 cm^{-1}. ν (CO–O) = 1712 cm^{-1}.

^{1}H NMR, δ (ppm): ($CDCl_3$):

5,05 (d, 1H, H-1, $J^2 = 6.98$ Hz), 4,31 (m, 2H, H-6), 4.07 (m, 1H, H-5), 3,68 (m, 1H, H-2), 3,30–3.45 (m, 2 H, H-2, H-4), 3,21 (s, 3H, OCH_3), 2.65 (s, 3H, 3OH). 2.23 (m, 2H, $CH_2CH_2CO_2$), 1.69 (m, 2H, $CH_2CH_2CO_2$), 1.32 (m, 24H, $(CH_2)_{12}$), 0.96 (t, 3H, CH_2CH_3, $J^3 = 7.06$ Hz).

^{13}C NMR ($CDCl_3$): 13.89, 22.55, 25.12, 28.75, 28.94, 31.56, 32.68, 33.92, 55.88, 60.73, 72.6133, 72.89, 79.04, 79.26, 104.23, 174.32.

Product (3)

$R_f = 0.14$ (MeOH/$CHCl_3$ 1/9). sulfuric acid. $T_f = 362$ °C. Chemical formula: $C_{25}H_{48}O_7$ (460). IR (KBr, solid): ν (OH) = 3540 cm^{-1}. ν (CH) = 2852, 2919 cm^{-1}. ν (CO–O) = 1712 cm^{-1}.

^{1}H NMR, δ (ppm): ($CDCl_3$):

5,03 (d, 1H, H-1, $J^2 = 7.05$ Hz), 4,33 (m, 2H, H-6), 4.09 (m, 1H, H-5), 3,77 (m, 1H, H-2), 3,29–3.48 (m, 2H, H-2, H-4), 3,25 (s, 3H, OCH_3), 2.75 (s, 3H, 3OH). 2.23 (m, 2H, $CH_2CH_2CO_2$), 1.67 (m, 2H, $CH_2CH_2CO_2$), 1.30 (m, 28H, $(CH_2)_{14}$), 0.96 (t, 3H, CH_2CH_3, $J^3 = 7.02$ Hz).

^{13}C NMR ($CDCl_3$): 14.01, 22.9, 25.23, 28.95, 29.12, 31.64, 32.57, 33.73, 55.8, 60.63, 72.71, 72.73, 78.74, 78.97, 103.45, 175.17).

References

1. C.T. Kresge, M.E. Leonowicz, W.J. Roth, J.C. Vartulli, J.S. Beck, Nature **359**, 710 (1992)
2. J.S. Beck, J.C. Vartuli, W.J. Roth, M.E. Leonowicz, C.T. Kresge, K.D. Schmitt, C.T.W. Chu, D.H. Olson, E.W. Sheppard, S.B. Mc Cullen, J.B. Higgins, J.L. Schlenker, J. Am. Chem. Soc. **114**, 10834–10843 (1992)
3. Y. Xia, R. Mokaya, Microporous Mesoporous Mater. **74**, 179–188 (2004)
4. J.-S. Cheng, J. Du, W. Zhu, Carbohydr. Polym. **88**, 61–67 (2012)
5. M. Cicuéndez, I. Izquierdo-Barba, M.T. Portolés, M. Vallet-Regí, Eur. J. Pharm. Biopharm. **84**, 115–124 (2013)
6. M. Moritz, M. Laniecki, Powder Technol. **230**, 106–111 (2012)
7. R. Hajian, S. Tangestaninejad, M. Moghadam, V. Mirkhani, I. Mohammadpoor-Baltork, A. R. Khosropour. J. Coord. Chem. **64**(23), 4134–4144 (2011)
8. A. Sayari, Chem. Mater. **8**, 1840–1852 (1996)
9. S. Nishihama, M. Murakami, N.Y. Igarashi, K. Yamamoto, K. Yoshizuka, Solvent Extr. Ion Exch. **30**, 724–734 (2012)
10. A. Benhamou, J.P. Basly, M. Baudu, Z. Derriche, R. Hamacha, J. Colloid Interface Sci. **404**, 135–139 (2013)
11. Y. Belmabkhout, A. Sayari, Adsorption **15**, 318–328 (2009)
12. B. Zhou, C.P. Wei, C.J. Peng, Y.C. Yu, J. Coord. Chem. **63**(10), 1752–1762 (2010)
13. X. Xie, D. Zhou, X. Zheng, W. Huang, W. Kangbing, Anal. Lett. **42**(4), 678–688 (2009)
14. Y. Sun, X.W. Liu, W. Su, Y. Zhou, L. Zhou, Appl. Surf. Sci. **253**, 5650–5655 (2007)
15. S. Giri, B.G. Trewyn, M.P. Stellmaker, V.S. Lin, Angew. Chem. Int. Ed. Engl. **44**(32), 5038–5044 (2005)
16. Y.S. Ooi, R. Zakaria, A.R. Mohamed, S. Bhatia, Appl. Catal. A Gen. **274**, 15 (2004)
17. S. Wang, T. Dou, Y. Li, Y. Zhang, X. Li, Z. Yan, J. Solid State Chem. **177**, 4800 (2004)

18. Y. de Xia, R. Mokaya, J. Mater. Chem. **14**, 863–870 (2004)
19. Y. de Xia, R. Mokaya, J. Mater. Chem. **14**, 3427–3435 (2004)
20. P. Prokesova, S. Mintova, J. Cejka, T. Bein, Microporous Mesoporous Materials **64**, 165 (2003)
21. P. Prokesova, S. Mintova, J. Cejka, N. Zilkova, A. Zukal, Microporous Mesoporous Materials **92**, 154 (2006)
22. Y. Li, J. Shi, H. Chen, Z. Hua, L. Zhang, M. Ruan, J. Yan, D. Yan, Microporous Mesoporous Materi.**60**, 51 (2003)
23. A.A. Twaiq Farouq, A.R. Mohamad, S. Bhatia. Fuel Process. Technol. **85**, 1283–1300 (2004)
24. S. Pei-Chun, W. Jung-Hui, M. Chung-Yuan, Catal. Today **93–95**, 365–370 (2004)
25. Z. Di, C. Yang, X. Jiao, J. Lia, W. Jinhu, D. Zhang, Fuel **104**, 878–881 (2013)
26. X. Li, B. Li, X. Junqing, Q. Wang, X. Pang, X. Gao, Z. Zhou, J. Piao, Appl. Clay Sci. **50**, 81–86 (2010)
27. C. Hea, P. Li, J. Chenga, HailinWanga, J. Li, Q. Li, Z. Hao, Appl. Catal. A Gen. **382**, 167–175 (2010)
28. C. Hea, J. Li, P. Li, J. Chenga, Z. Hao, Z.-P. Xu, Appl. Catal. B Environ. **96**, 466–475 (2010)
29. D.W. Park, J.S. Kim, J.H. Seung, H.S. Kim, W.S. Kim, Biotechnol. Lett. **23**, 1947–1952 (2001)
30. H.G. Park, J.H. Do, H.N. Chang, Biotechnol. Bioprocess. Eng. **8**, 1–8 (2003)
31. J.F. Kennedy, H. Kumar, P.S. Panesar, S.S. Marwaha, R. Goyal, A. Parmar, S.J. Kaur, Chem. Technol. Biotechnol. **81**, 866–876 (2006)
32. J. Liang, W. Zeng, P. Yao, Y. Wei, Adv. Biol. Chem. **2**, 226–232 (2012)
33. M. Terreni, R. Salvetti, L. Linati, R. Fernandez-Lafuente, G. Fernández-Lorente, A. Bastida, M. José Guisan, Carbohydr. Res. **337**, 1615–1621 (2002)
34. W. Muramatsu, Y. Takemoto, J. Org. Chem. **78**, 2336–2345 (2013)
35. T. Ogawa, Y. Takahashi, M. Matsui, Carbohydr. Res. **102**, 207–215 (1982)
36. X. Li, Z. Li, P. Zhang, H. Chen, S. Ikegami, Synth. Commun. Int. J. Rapid Commun. Synth. Org. Chem. **37**, 2195–2202 (2007)
37. R. Engel, J.I. Rizzo, C. Rivera, M. Ramirez, M.L. Huang, H. Weiss, O. Adelkader, C. Capodiferro, V. Behaj, M. Thomas, J.F. Engel, Chem. Phys. Lipids **158**, 61–69 (2009)
38. J.I. Cohen, S. Castro, J.A. Han, V. Shteto, R. Engel, Heteroat. Chem. **11**, 546–555 (2000)
39. J. Fabian, T. October, A. Cherestes, R. Engel, Synlett **1997**, 1007–1009 (1997)
40. T. Strekas, R. Engel, K. Locknauth, J. Cohen, J. Fabian, Arch. Biochem. Biophys. **364**, 129–131 (1999)
41. J.I. Cohen, L. Traficante, P.W. Schwartz, R. Engel, Tetrahedron Lett. **39**, 8617–8620 (1998)
42. A. Sakthivel, S.J. Huang, W.H. Chen, Z.H. Lan, K.H. Chen, H.P. Lin, C.Y. Mou, S.B. Liu, Adv. Funct. Mater. **15**, 253–258 (2005)
43. T. Maugard, M. Remaud-Simeon, D. Petre, P. Monsan, Tetrahedron **76**, 7629–7634 (1997)
44. H.H. Sung, M.H. Nguyen, H.L. Sang, Y.M. Koo, Bioprocess Biosyst. Eng. **33**, 63 (2010)
45. Y. Xia, R. Mokaya, Microporous Mesoporous Mater.**68**, 1–10 (2004)
46. E.P. Barrett, L.G. Joyner, P. Halenda, J. Amer. Chem. Soc. **73**, 373–380 (1951)
47. Z.-Q. Duan, W. Du, D.-H. Liu, Bioresour. Technol. **101**, 2568–2571 (2010)
48. Z.-Q. Duan, W. Du, D.-H. Liu, Bioresour. Technol. **102**, 11048–11050 (2011)
49. Y. Liu, X. Zhang, H. Tan, Y. Yan, B.H. Hameed, Process Biochem. **45**, 1176–1180 (2010)
50. J.M. Fraile, E. García-Bordejé, L. Roldán, J. Catal. **289**, 73–79 (2012)
51. L.A.S. Gorman, J.S. Dordick, Biotechnol. Bioeng. **39**, 392–397 (1992)
52. S.R. Lipsky, W.J. McMurray, J. Chromatogr. **279**, 59–68 (1983)
53. H. Utsugi, H. Horikoshi, T. Matsuzawa, J. Colloid Interface Sci. **50**, 154–161 (1975)
54. H. Landmesser, H. Kosslick, W. Storek, R. Fricke, Solid State Ion. **101**, 271–277 (1997)
55. K. Schumacher, P.I. Ravikovitch, A. Du Chesne, A.V. Neimark, K.K. Unger, Langmuir **16**, 4648–4654 (2000)
56. H. Ji, Y. Fan, W. Jin, C. Chen, X. Nanping, J. Non-Cryst. Solids **354**, 2010–2016 (2008)
57. S. Hitz, R. Prins, J. Catal. **168**, 194–206 (1997)
58. N. Gokulakrishnan, A. Pandurangan, P.K. Sinha, J. Mol. Catal. A: Chem. **263**, 55–61 (2007)
59. C. Alípio Carmo Jr, L.K.C. de Souza, C.E.F. da Costa, E. Longo, R. José Zamian, R.G.N. da Filho, Fuel **88**, 461–468 (2009)
60. S. Ajaikumar, A. Pandurangan, J. Mol. Catal. A: Chem. **266**, 1–10 (2007)
61. S. Bellahouel, E. Belhadj, H. Sekkiou, R. Hamacha, N. Kambouche, A. Derdour, A. Bengueddach, Arab. J. Chem. **4**, 355–359 (2011)
62. J. Barrault, S. Bancquart, Y. Pouilloux, C R Chimie. **7**, 593–599 (2004)